Noname manuscript No.
(will be inserted by the editor)

A fundamental link between steady asymmetry and separation length in the wake of a 3D square-back body

En-Chi Hsu · Luc Pastur · Olivier Cadot · Vladimir Parezanović

Received: date / Accepted: date

Abstract Suction applied at the base of a square-back Ahmed body is shown to create a global effect on the wake, reducing the recirculating bubble length and increasing the base drag. Weak suction causes a small shortening of the bubble and intensifies the steady reflectional symmetry breaking (RSB) mode present in the horizontal direction. Stronger suction significantly suppresses the RSB mode, indicating that the steady asymmetric instability does not bear a highly curved bubble. The stabilized wake experiences very low frequency oscillations in the horizontal direction together with a well synchronized shedding mode in the vertical direction.

Keywords 3D Bluff Body · Bistable Wake · Flow control · Base suction

The wake which develops behind squareback bodies experiences a steady reflectional symmetry breaking (RSB) in the laminar regime leading to the so-called RSB mode. It persists in the turbulent regime through a permanent wake asymmetry and bi-stable dynamics up to Reynolds numbers as large as few million (Grandemange et al., 2013). There have been many attempts to control the RSB mode, the results of which can be divided into two categories, both suppressing the bi-stable dynamics. Barros et al. (2017) was the first to report that the suppression of the bi-stability in the horizontal direction can be accompanied by an increase of asymmetry in the vertical direction. For this kind of "waterbed effect", the direction of the asymmetry has rotated without any clear stabilization of the mode. The Simultaneous reduction of asymmetry in both directions has been achieved with a vertical control cylinder placed at the center of the recirculating bubble and a body with a deep rear cavity (see Evrard et al. (2016) and reference therein). The drag decrease found for these cases has stimulated active flow control experiments targeting symmetric flows (Li et al., 2016; Brackston et al., 2016; Haffner et al., 2020). The present work is strongly connected to the Lorite-Díez et al. (2020) experiment who investigated rear slits steady blowing. Their main result is equivalent to the bubble elongation and drag decrease obtained for 2D bodies (Bearman, 1967). The initial bubble growth is also accompanied by a small reduction in the intensity of the RSB mode, without stabilisation. In this letter, it will be shown that base suction, which is known to increase drag (Bearman, 1967; Brogna and Hawks, 1978), is able to efficiently suppress the RSB mode by shortening the bubble.

Experiments are conducted in an Eiffel-type wind-tunnel having a test section 400 mm-wide by 390 mm-high, with open lateral sides. The square-back model (Fig. 1), has dimensions of $l = 292$ mm, $w = 98$ mm and $h = 72$ mm, with a ground clearance of $c/h = 0.278$. It is supported by four cylinders of 7 mm in diameter. The uniform flow speed

E.C. Hsu · L. Pastur
Institute of Mechanical Sciences and Industrial Applications, ENSTA-Paris, Institut Polytechnique de Paris, 828 Bd des Maréchaux, F-91120 Palaiseau, France.

O. Cadot
School of Engineering, University of Liverpool, Liverpool L69 3GH, UK.

V. Parezanović
Khalifa University of Science and Technology, P.O. Box 127788, Abu Dhabi, UAE.
E-mail: vladimir.parezanovic@ku.ac.ae

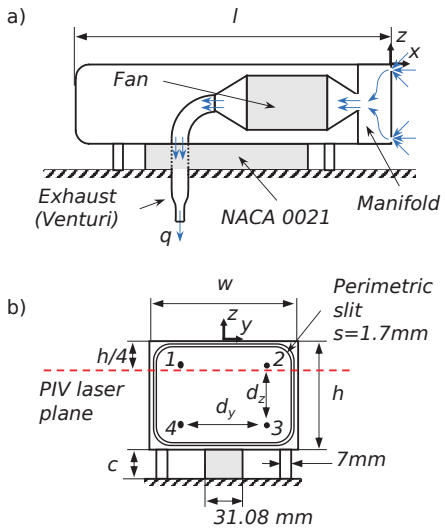

Fig. 1 Side (a) and back (b) view of the experimental model.

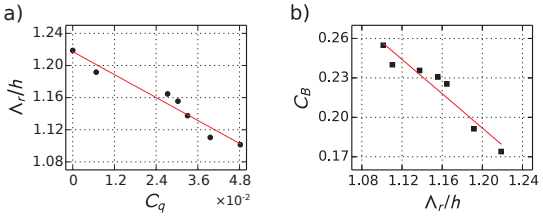

Fig. 2 Characteristic size of the recirculating bubble Λ_r/h versus the suction coefficient C_q (a). Base drag coefficient C_B versus Λ_r/h (b).

in the wind tunnel is set to $U_\infty = 13.7$ m.s^{-1}, yielding a Reynolds number $Re = U_\infty h/\nu \approx 6.5 \times 10^4$, where ν is the air kinematic viscosity. The flow frequencies f are expressed as Strouhal numbers $St = fh/U_\infty$.

A 10-blade ducted fan, housed within the model, provides air suction through the 1.7 mm perimetric slit at the base, the center of which is located 5.8 mm away from the nearest trailing edge. The fan is 50 mm in diameter, rated at 4000 RPM per volt. The air sucked at the base is expelled through the exhaust pipe of radius $r_e = 12.35$ mm (Fig. 1a). A Venturi tube estimates the volumetric suction flow rate q that is then expressed as the coefficient $C_q = q/U_\infty hw$ using the base surface hw and the uniform wind speed U_∞. The exhaust pipe causes high blockage which is considerably reducing the intensity of the under-body flow. This case is similar to a ground clearance smaller than the threshold necessary to observe the RSB mode (Cadot et al., 2015). Therefore, the exhaust pipe is streamlined by a NACA 0021 profile, which increases the under-body flow intensity and recovers the RSB mode dynamics. The same technique was also used in Cadot et al. (2020).

Pressure measurements are obtained using a *Scanivalve ZOC22B/32* pressure scanner, with a sampling frequency of 200 Hz. Pressures p_i are measured at four locations at the base (Fig. 1b), separated by $d_y = 40$ mm and $d_z = 57$ mm. The pressure coefficient is defined as $c_p = 2\frac{p-p_\infty}{\rho U_\infty^2}$, where p_∞ is the static pressure of the reference Pitot tube providing the value of U_∞. The four local measurements are used to assess the mean base drag coefficient as:

$$C_B = -\frac{1}{4}\sum_{i=1}^{4}\overline{c_{pi}}, \tag{1}$$

and the components of the non-dimensional pressure gradient as:

$$g_y = \frac{(c_{p_2} - c_{p_1}) + (c_{p_3} - c_{p_4})}{2d_y/h}, \tag{2}$$

$$g_z = \frac{(c_{p_1} - c_{p_4}) + (c_{p_2} - c_{p_3})}{2d_z/h}. \tag{3}$$

The near wake velocity fields are measured using Particle Image Velocimetry (PIV) in the $z = -h/4$ plane (Fig. 1b). The PIV system uses a dual pulse laser (Nd:YAG, 2 x 135mJ, 4ns) synchronized with a *FlowSense EO*, 4 Mpx CCD camera. Statistics are performed over 800 velocity fields sampled at 1 Hz. Velocities were computed from an interrogation window of 16 × 16 pixels with an overlap of 50%, resulting into a spatial resolution of 1% of the body's height. The characteristic size of the recirculating flow Λ_r is the distance from the base to the furthest location where the mean streamwise velocity is equal to zero in the $z = -h/4$ plane. It is obviously smaller than that obtained from the plane $z = -h/2$ and referred to as L_r in Grandemange et al. (2013); Lorite-Díez et al. (2020). We estimate L_r to be 15% (at $h/4$) larger than Λ_r.

Fig. 2(a) shows that the characteristic size of the recirculating bubble decreases as an affine function of the suction coefficient. The suction is equivalent to a line sink flow whose momentum decays inversely with the distance. The maximum slit-induced velocity at the nearest trailing edge, classically estimated from the inviscid source/sink flow model, is less than 6% of the freestream velocity U_∞, therefore, the local interaction with the separated shear layers is considered as negligible. The dominant mechanism is more likely based on the

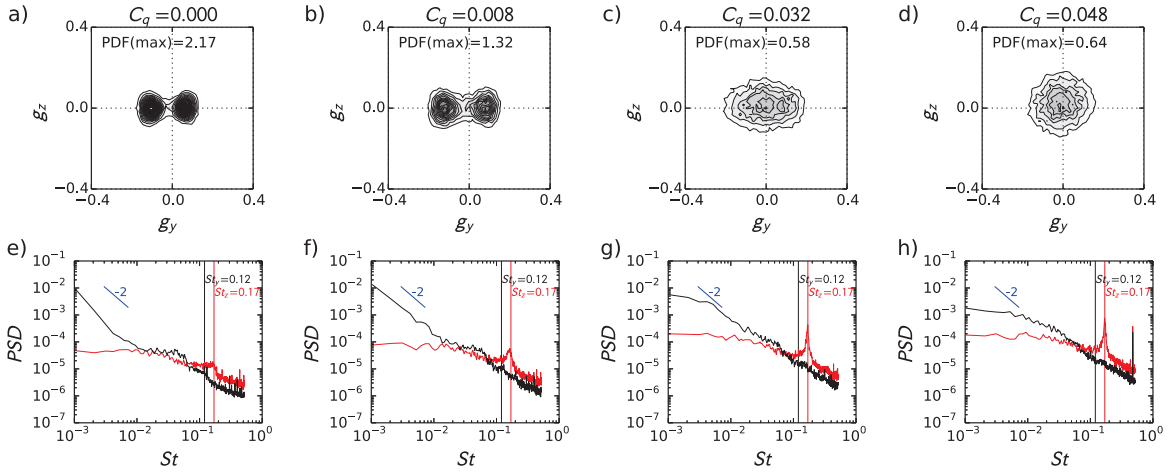

Fig. 3 Histograms (a-d), and power spectral density (PSD) (e-h) of the g_y (black) and g_z (red) pressure gradients for: (a,e) $C_q = 0$, (b,f) $C_q = 0.008$, (c,g) $C_q = 0.032$, and (d,h) $C_q = 0.048$. The normalized PDF is presented by grey-scale map using 20 levels in a common range, and the indicated maximum value.

removal of fluid mass from the near wake, which forces the bubble to establish a new equilibrium with a reduced length. This global effect results from a budget of mass fluxes feeding and emptying the recirculating region as first introduced by Gerrard (1966) and adapted by Lorite-Díez et al. (2020) to base bleed. Similarly to the *mass regime* in the latter, where fluid injected with negligible momentum inside the recirculating bubble leads to its inflation, fluid extraction by base suction leads to bubble deflation. The assumption of negligible local interaction with the shear layers should be valid for larger flow rate than that for fluid injection through the slit as a consequence of the non-reversibility of the Navier-Stokes equations (Batchelor, 2002). The direct effect of the bubble size reduction on the base drag is clearly observable in Fig. 2(b) and may be interpreted as a base pressure reduction due to larger flow curvature around the recirculation region as the bubble shrinks (see Lorite-Díez et al. (2020) for further details).

The statistics of the base pressure gradient are represented by the joint probability density function (PDF) of the gradient components g_y and g_z, shown for four distinct values of C_q in Fig. 3(a-d). The horizontal RSB mode with the distinct bi-modal probability distribution in the g_y direction, dominates the flow at $C_q = 0$ (Fig. 3a). At a low suction rate of $C_q = 0.008$ (Fig. 3b) the pressure gradient encompasses a wider range of possible values. This first change indicates an intensification of the RSB mode as the recirculating bubble is shortened. It seems to mirror the weakening of the RSB mode reported by Lorite-Díez et al. (2020) as the recirculating bubble is elongated. A further increase in suction at $C_q = 0.032$ yields a very drastic change, with the disappearance of the bi-modal probability distribution, and an additional increase in the maximum permissible g_y values (Fig. 3c). Finally, for the highest value of $C_q = 0.048$, the PDF transforms into an isotropic distribution (Fig. 3d).

The wake survey of Grandemange et al. (2013); Lorite-Díez et al. (2020) showed the presence of 2 periodic modes at $St_y = 0.12$ and $St_z = 0.17$. These modes are however less pronounced in the dynamics of the base pressure distribution (Brackston et al., 2016). The spectra for both base pressure gradient components are shown in Fig. 3(e-h). The frequencies $St_y = 0.12$ and $St_z = 0.17$ are indicated with the straight lines. The two periodic vortex shedding modes in the horizontal and vertical directions are barely distinguishable. However, as the suction is increased, we see a strong intensification of the vertical mode as indicated by the emergent peak in the spectra of g_z, whose maximum is 50 times larger for $C_q = 0.048$ (Fig. 3h), compared to the baseline (Fig. 3e). The horizontal mode at $St_y = 0.12$ (Fig. 3f) seems to disappear completely for $C_q \geq 0.032$ (Fig. 3g). Additional thin peaks in the spectra as that around $St_y = 0.45$ in Fig. 3(h) originate from the suction turbine.

The RSB mode dynamics are characterized by a power law in the spectrum at very low frequencies (Grandemange et al., 2013) with a slope close to -2 observable for the y component of the gradient in Fig. 3. This is due to the bi-stable dynamics of random switches between the two states evidenced in the joint PDF, and appears as a universal feature of multi-stable signals in turbulent flows (Herault et al., 2015). We can see in Fig. 3 that a

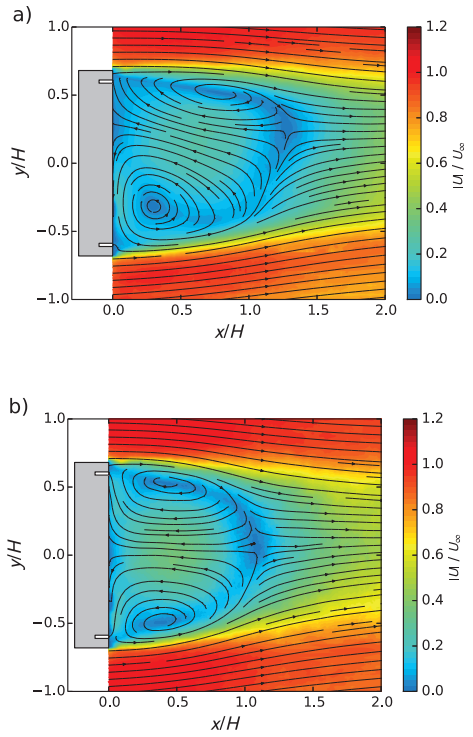

Fig. 4 Conditionally averaged velocity fields of the P state, based on the spatial integral of instantaneous velocity v (see text) for (a) $C_q = 0$, and (b) $C_q = 0.048$. White rectangles at the base of the bluff body indicate the exact size and locations of the suction slits.

low suction at $C_q = 0.008$ (Fig. 3f) increases the energy at low frequencies of g_y, which corroborates the primary effect of a small intensification of the RSB mode for weak bubble shortening. However, a low frequency cut-off appears for $C_q \geq 0.032$ that flattens the spectra (Fig. 3g). This affects significantly the initial power law, although the g_y dynamics are still dominated by low frequencies. The spectra analysis reveals that the natures of the horizontal and vertical fluctuations in the isotropic joint PDF at $C_q = 0.048$ (Fig. 3h) are actually drastically different, g_z fluctuations are dominated by a vertical shedding mode at $St_z = 0.17$ while g_y fluctuations are associated with oscillations in the horizontal plane over a continuum of low frequencies.

The effect of the asymmetry suppression is clear in Fig. 4, showing the conditional averaging of the velocity fields such that for the y-component of the velocity v, $\iint_\Omega v dxdy > 0$ where Ω is the full PIV domain. It provides the so-called P state first reported in Grandemange et al. (2013) for the baseline at $C_q = 0$ (Fig. 4a), which leads to a rather symmetric wake at $C_q = 0.048$ (Fig. 4b). In addition, there is no evidence of local interactions between the slit suction and the free shear layers near separation, thus excluding flow modifications by suction momentum and confirming the global effect mechanism of the bubble shortening.

To conclude, weak base suction causes a small bubble shortening and intensifies the RSB mode, while higher suction values shorten the bubble progressively more and suppress the RSB mode. The first case is reminiscent of the initial bubble increase and the concomitant RSB mode damping in Lorite-Díez et al. (2020). This is likely a general consequence of a small bubble reduction which brings the global mode closer to the base, increasing the base pressure gradient (Parezanović and Cadot, 2012). For larger shortening of the bubble, the RSB mode is suppressed and the wake is dominated by low frequency oscillations in the horizontal direction, and a well synchronized shedding mode in the vertical direction. We hypothesize that the steady asymmetric instability does not bear a highly curved bubble, which is the case when the bubble is reduced.

It is well known in the literature that curvature is stabilizing the development of mixing layers (Castro and Bradshaw, 1976). However, it is acknowledged to rather affect unsteady instabilities such as the Kelvin-Helmholtz instabilities. The stabilization of a steady asymmetric instability of a recirculation region bounded by highly curved mixing layers appears as a new result that would deserve further theoretical investigations.

Acknowledgements The authors would like to acknowledge the invaluable help of Thierry Pichon in getting the experimental setup operational. This work has been supported by the Khalifa University of Science and Technology under Award No(s). FSU-2018-21 and CIRA-2019-025.

References

Barros D, Borée J, Cadot O, Spohn A, Noack BR (2017) Forcing symmetry exchanges and flow reversals in turbulent wakes. Journal of Fluid Mechanics 829

Batchelor G (2002) An introduction to fluid dynamics. Cambridge University Press

Bearman P (1967) On vortex street wakes. Journal of Fluid Mechanics 28(4):625–641

Brackston RD, García De La Cruz J, Wynn A, Rigas G, Morrison JF (2016) Stochastic modelling and feedback control of bistability in a

turbulent bluff body wake. Journal of Fluid Mechanics 802:726–749, DOI 10.1017/jfm.2016.495
Brogna SJ, Hawks RJ (1978) Effect of base suction on subsonic drag of bluff bodies. Journal of Aircraft 15(7):443–444
Cadot O, Evrard A, Pastur L (2015) Imperfect supercritical bifurcation in a three-dimensional turbulent wake. Physical Review E 91(6):063005
Cadot O, Almarzooqi M, Legeai A, Parezanović V, Pastur L (2020) On three-dimensional bluff body wake symmetry breaking with free-stream turbulence and residual asymmetry. Comptes Rendus Mécanique 348(6-7):509–517
Castro IP, Bradshaw P (1976) The turbulence structure of a highly curved mixing layer. Journal of Fluid Mechanics 73(2):265–304
Evrard A, Cadot O, Herbert V, Ricot D, Vigneron R, Délery J (2016) Fluid force and symmetry breaking modes of a 3D bluff body with a base cavity. Journal of Fluids and Structures 61:99–114
Gerrard J (1966) The mechanics of the formation region of vortices behind bluff bodies. Journal of Fluid Mechanics 25(02):401–413
Grandemange M, Gohlke M, Cadot O (2013) Turbulent wake past a three-dimensional blunt body. Part 1. Global modes and bi-stability. Journal of Fluid Mechanics 722:51–84
Haffner Y, Borée J, Spohn A, Castelain T (2020) Mechanics of bluff body drag reduction during transient near-wake reversals. Journal of Fluid Mechanics 894, DOI 10.1017/jfm.2020.275
Herault J, Pétrélis F, Fauve S (2015) $1/f^{\alpha}$ low frequency fluctuations in turbulent flows. Journal of Statistical Physics 161(6)
Li R, Barros D, Borée J, Cadot O, Noack BR, Cordier L (2016) Feedback control of bimodal wake dynamics. Experiments in Fluids 57(10):158
Lorite-Díez M, Jiménez-González J, Pastur L, Martínez-Bazán C, Cadot O (2020) Experimental analysis of the effect of local base blowing on three-dimensional wake modes. Journal of Fluid Mechanics 883
Parezanović V, Cadot O (2012) Experimental sensitivity analysis of the global properties of a two-dimensional turbulent wake. Journal of Fluid Mechanics 693:115–149